Pacific Graphics 2014
J. Keyser, Y. J. Kim, and P. Wonka
(Guest Editors)

Volume 33 (2014), Number 7

Sky Based Light Metering for High Dynamic Range Images

Supplemental Materials

Yulia Gryaditskaya[1], Tania Pouli[1,2], Erik Reinhard[1,2] and Hans-Peter Seidel[1]

[1]Max-Planck Institute for Informatics, Saarbrücken, Germany
[2]Technicolor Research and Innovation, Rennes, France

Abstract

To aid in reproducing our work, the supplemental materials for Sky Based Light Metering for High Dynamic Range Images contain supporting information on the models that we have adopted (zenith luminance models and overcast sky type definitions). We also present additional results to demonstrate the robustness of our algorithm.

A. Background

This section describes in more detail the parametric sky models as well as the zenith luminance models that our algorithm employs. Although most of the information in this section is part of existing literature, we feel that its inclusion will aid in implementing our method as well as in motivating our choices.

When sunlight enters the atmosphere, it interacts with particles and molecules before reaching ground level. Small particles cause Rayleigh scattering (which leads to blue skies and a yellow sun), whereas larger molecules create Mie scattering, which is not strongly wavelength dependent but leads to haze. The latter is often described with a single parameter, called turbidity [McC76]. The luminance distribution of the sky dome thus depends on atmospheric conditions as well as the position of the sun. Various models exist that predict this distribution. In our work, we use the Perez sky model as a prior, which was shown to out-perform competing algorithms [IM94]. It allows us to infer the luminance arriving from the zenith, based on the sky region visible in the input HDR image.

A.1. The Relative All-Weather Perez Sky Model

The model introduced by Perez et al. [PSM93] consists of two factors. The first factor describes vertical gradations of luminance values and is therefore called the gradation function:

$$f_{\text{grad}}(\theta_p, a, b) = 1 + a\exp(b/\cos\theta_p), \tag{1}$$

where θ_p is the zenith angle of the considered sky element (see Figure 2), a and b are two parameters which describe sky properties. The first parameter a corresponds to darkened ($a > 0$) or lightened horizon regions ($a < 0$), which is indicative of whether the sky is overcast or not. The second parameter $b \in [-1, 0]$ refers to changes of the luminance gradient near horizon. This factor describes sky luminances away from the sun.

The second factor describes the influence of the sun on the sky and is given by the indicatrix function:

$$f_{\text{ind}}(\gamma_p, c, d, e) = 1 + c\exp(d\gamma_p) + e\cos^2\gamma_p, \tag{2}$$

where γ_p is the angle between a sky element and the position of the sun (Fig. 2) and c, e, d are parameters describing the sky appearance near the sun. Parameter $c \geq 0$ is proportional to the luminance of the circumsolar region, while d is its width. Finally, e accounts for the relative intensity of backscattered light. Combining these parameters into a vector $\vec{\rho} = (a, b, c, d, e)$, Perez's full model is then the product of these two factors:

$$f(\theta_p, \gamma_p, \vec{\rho}) = f_{\text{grad}}(\theta_p, a, b) f_{\text{ind}}(\gamma_p, c, d, e) \tag{3}$$

The values returned by the Perez sky model are not absolute and can be normalized to any desirable range of values, using a known luminance value of any sky element. Typically, the zenith luminance l_z is used:

$$l_p = l_z \frac{f(\theta_p, \gamma_p, \vec{\rho})}{f(0, \theta_s, \vec{\rho})}, \tag{4}$$

where $f(0, \theta_s, \vec{\rho})$ is the relative luminance at the zenith, predicted by (3), as in this case the zenith angle θ_p of the sky element is equal to zero, and the angle of the sky element with

Type	Gradation	Indikatrix	a	b	c	d	e	B	C	D	E	D_v/E_v
1	II	2	1.1	-0.8	2	-1.5	0.15	12.23	3.57	0.57	44.27	0.22
2	I	2	4.0	-0.7	2	-1.5	0.15	12.35	3.68	0.59	50.47	0.18
3	III	1	0.0	-1.0	0	-1.0	0.00	42.59	1.00	0.00	0.00	0.20
4	II	1	1.1	-0.8	0	-1.0	0.00	48.30	1.00	0.00	0.00	0.10
5	I	1	4.0	-0.7	0	-1.0	0.00	54.63	1.00	0.00	0.00	0.10

Table 1: *Typical parameters for five standard overcast sky types.*

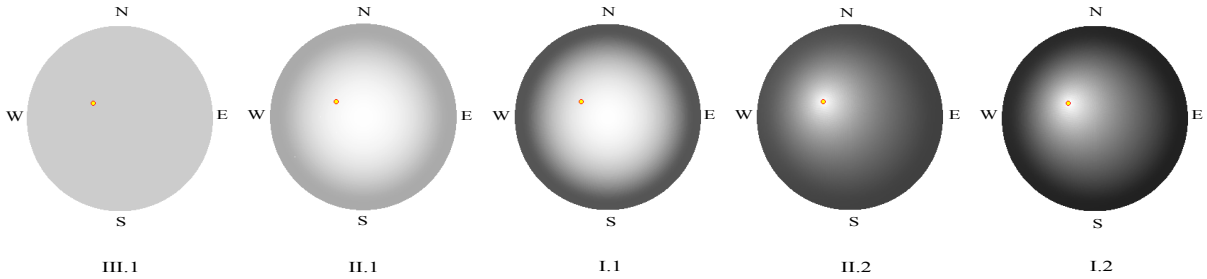

Figure 1: *Relative distribution of luminance over the sky dome for each of the five overcast sky types. The yellow circle denotes sun position.*

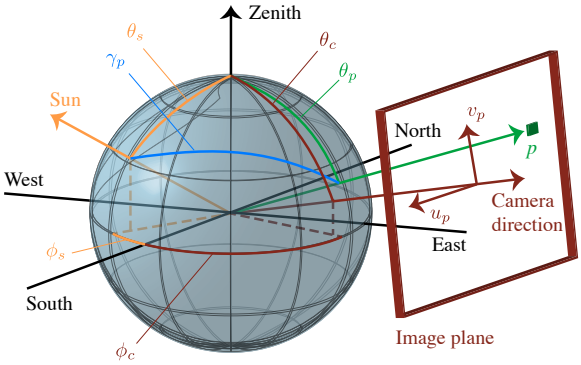

Figure 2: *Angles defining the position of the sun, a camera and a sky pixel p in the image.*

the sun γ_p is equal to the sun zenith angle θ_s (see Figure 2). The five parameters in Perez's model directly relate to turbidity t, especially for relatively low turbidities ($t \in [2,6]$) that describe atmospheres that are between clear and thin fog [PSS99];

$$\tilde{\rho}^T = \begin{bmatrix} t \\ 1 \end{bmatrix}^T \begin{bmatrix} 0.179 & -0.355 & -0.023 & 0.121 & -0.067 \\ -1.463 & 0.428 & 5.325 & -2.577 & 0.370 \end{bmatrix} \quad (5)$$

Given this relation, we will use $f(\theta_p, \gamma_p, \rho)$ and $f(\theta_p, \gamma_p, t)$ interchangeably, but note that turbidity only describes clear to hazy skies; it is not appropriate for overcast skies.

A.2. Recovery of Camera Parameters

The sky area in the image can be a rich source of information, especially given knowledge of the luminance distribution $f(\theta_p, \gamma_p, t)$ of the sky dome. This can for instance be used to recover camera parameters such as focal length f_c, zenith angle θ_c and azimuth angle ϕ_c [LNE08, LGE10] by minimizing the difference between observed sky pixel values and the parametric luminance distribution of the sky dome. To compare image intensities with the sky luminance distribution two operations should be performed. First, the relation of pixel in position (u_p, v_p) in the image and the corresponding sky element p in the sky dome should be set (see Figure 2). This is obtained by expressing the sky element zenith and azimuth angles in terms of the camera parameters and pixel coordinates. The zenith angle θ_p of the sky element and its angle with the sun γ_p are [LGE10]:

$$\theta_p = \cos^{-1}\left(\frac{v_p \sin\theta_c + f_c \cos\theta_c}{\sqrt{f_c^2 + u_p^2 + v_p^2}}\right) \quad (6)$$

$$\gamma_p = \cos^{-1}\left(\cos\theta_s \cos\theta_p + \sin\theta_s \sin\theta_p \cos(\phi_p - \phi_s)\right), \quad (7)$$

where ϕ_s is the sun azimuth angle and the sky element azimuth angle ϕ_p is found from the equation:

$$\tan(\phi_p) = \frac{f_c \sin\phi_c \sin\theta_c - u_p \cos\phi_c - v_p \sin\theta_c \cos\phi_c}{f_c \cos\phi_c \sin\theta_c + u_p \sin\phi_c - v_p \cos\theta_c \cos\phi_c}.$$

Now, Equation (3) can be expressed in terms of camera parameters and pixel coordinates:

$$f(\theta_p, \gamma_p, \rho) = g(u_p, v_p, \theta_c, \phi_c, f_c, \theta_s, \phi_s, \rho), \quad (8)$$

Symbol	Meaning
θ	Zenith angle
ϕ	Azimuth angle
Subscript $_c$	Referring to the camera
Subscript $_p$	Referring to a sky element in the image
Subscript $_s$	Referring to the sun
γ_p	Angle between the sun and a sky element
(u_p, v_p)	Coordinates of sky element in image
f_c	Focal length of the camera
ζ	Sun elevation angle
t	Sky turbidity
l_z	Relative zenith luminance
L_z	Absolute zenith luinance
ξ	Absolute scaling factor

Table 2: *Symbols used in the description of the algorithm.*

Second, the luminance values produced by g should be normalized to the range of the intensities in the image. For this, we use Equation (4). As we are not interested in absolute values and the zenith can rarely be observed in the image, an optimization is also performed for the zenith luminance value l_z, which is in this case relative to luminance values in the image l_p.

A.3. Absolute Zenith Luminance Models

We are interested in finding absolute values for all the pixels in the image. This requires the aid of the aforementioned sky luminance distribution models, although this can only give us relative values. There is, however, one position in the sky with special relevance, which is the zenith. There exist several models which correlate the luminance arriving from the zenith to the solar elevation as well as turbidity for cloudless skies [KNNS84, PSS99, SG00] as well as for overcast skies [SGC01]. The time of year and the luminous clearness index of the sky is also indicative of zenith luminance [SG01].

For clear skies, we selected zenith luminance models from Karayel et al. [KNNS84] and Soler and Gopinathan [SG00], as these were found to perform well in a comparative study [ZWP07]. Zenith luminance L_z^{Karayel} can be computed from turbidity t and sun elevation angle ζ [KNNS84]:

$$L_z^{\text{Karayel}} = (1.376t - 1.81)\tan(\zeta) + 0.38, \qquad (9)$$

where t is turbidity and ζ is the sun elevation angle. Soler and Gopinathan [SG00] propose to fit fifth order polynomials to measured data as function of sun elevation angle ζ:

$$L_z^{\text{Soler}} = \exp\left(\sum_{i=0}^{5} k_i \zeta^i\right) \qquad (10)$$

where k_i are coefficients. They derived a set of five models for various different conditions. The parameters for each of these models are given in Table 3.

For overcast skies, models of zenith luminance can be derived for different sky types ranging from completely overcast to near overcast [KPD98, SGC01]. In particular, Kittler et al. [KPD98] distinguish five different types of overcast skies. Zenith luminance of a given sky type can be found using [CIE03]:

$$L_z^{\text{overcast}} = \frac{D_v}{E_v}\left(\frac{B(\sin(\zeta))^C}{(\cos(\zeta))^C} + E\sin(\zeta)\right), \qquad (11)$$

where D_v is diffuse sky illuminance, E_v is extraterrestrial horizontal illuminance, ζ, as previously, is the sun elevation angle, and B, C and E are parameters determined by the given sky type.

B. Further Algorithm Details

B.1. Images with clear skies

We find that including turbidity t in the optimization provides a significant advantage over fixing turbidity to the constant value of $t = 2.17$, which is the CIE-defined turbidity for a clear sky [CIE03]. The results for different types of Soler et al. [SG00] zenith luminance models are shown in Fig. 3, and aggregated in Tables 4 and 5. It could be seen that our optimization algorithm is sufficiently stable to include turbidity in the calculations.

The mean and standard deviation of errors obtained using our weighted combination of Karayel [KNNS84] and Soler [SG00] are listed in Table 6. As all three Soler models produce comparably good results, we chose the model $Soler_t$ because of its lower standard deviation.

B.2. Images with overcast skies

B.2.1. Overcast Sky Types

Overcast skies can be classified into one of five general types [KPD98]. Moreover, these types can be described in terms of the five sky parameters a, b, c, d, e from Perez's sky model [PSM93]. The parameters a and b define the representation of gradation function, which is defined in the main paper. Here, the types of gradation function are denoted by Roman numerals. The parameters c, d and e in turn define the representation of the indikatrix function (also defined in the main paper), whose types are denoted by Arabic numbers. The values of the five parameters describing each of five sky types can be found in Table 1 and the relative luminance distribution for each sky type is shown in Figure 1. The discription of these five sky types is as follows:

I.1 Sky with steep luminance gradation towards zenith and azimuthal uniformity

II.1 Sky moderately graded with azimuthal uniformity

III.1 Sky of uniform luminance

Model	Description	k_0	$10^2 k_1$	$10^3 k_2$	$10^4 k_3$	$10^6 k_4$	$10^9 k_5$
Soler13_1	Zenith luminance 15–min means	-0.68260	9.922	-5.16	1.44300	1.8918	9.3644
Soler13_2	Zenith luminance at every 5° interval of ζ	-0.60647	8.594	-4.44	1.29610	1.7942	9.4016
$\text{Soler}_{t<3}$	Turbitidy $t < 3$	-0.61538	8.580	-4.48	1.26190	1.6824	8.54789
$\text{Soler}_{3<t<5}$	Turbidity $3 < t < 5$	-0.60879	9.129	-4.52	1.22350	1.5829	7.84640
$\text{Soler}_{t>5}$	Turbidity $t > 5$	-0.58487	0.023	-3.88	0.99654	1.2851	6.55570

Table 3: *Coefficients for 5th degree polynomial zenith luminance models from Soler and Gopinathan [SG00].*

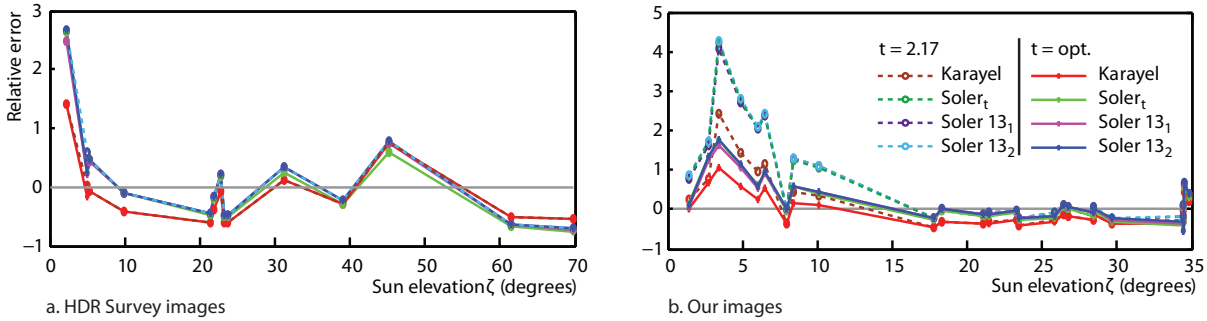

Figure 3: *Relative errors for images with clear sky regions from the HDR Survey [Fai07] (left) and from our own dataset (right).*

Zenith Lum. Model	$\mu(\lvert\delta\rvert)$			
	$t = 2.17$	t optimized		
	all ζ	all ζ	$\zeta < 15$	$\zeta > 15$
Karayel	0.459	0.469	0.515	0.450
Soler_t	0.586	0.563	0.863	0.442
Soler13_1	0.577	0.554	0.815	0.449
Soler13_2	0.795	0.572	0.875	0.450

Table 4: *Mean μ of relative errors magnitudes $\lvert\delta\rvert$ for images from the HDR Photographic Survey.*

Zenith Lum. Model	$\mu(\lvert\delta\rvert)$			
	$t = 2.17$	Opt. t		
	all ζ	all ζ	$\zeta < 15$	$\zeta > 15$
Karayel	0.503	0.354	0.416	0.319
Soler_t	0.759	0.416	0.769	0.218
Soler13_1	0.745	0.396	0.724	0.211
Soler13_2	0.773	0.413	0.768	0.212

Table 5: *Mean values μ of relative error magnitudes $\lvert\delta\rvert$ in our clear-sky image collection.*

I.2 Sky with steep luminance gradation towards zenith and slight brightening towards the sun

II.2 Sky moderately graded with slight brightening towards the sun

Algorithm	HDR Survey		Our data	
	$\mu(\lvert\delta\rvert)$	$\sigma(\lvert\delta\rvert)$	$\mu(\lvert\delta\rvert)$	$\sigma(\lvert\delta\rvert)$
Soler_t	0.440	0.334	0.309	0.251
Soler13_1	0.445	0.345	0.305	0.255
Soler13_2	0.445	0.346	0.307	0.256

Table 6: *Mean μ and standard deviation σ of relative error magnitudes $\lvert\delta\rvert$ for images with clear sky regions, when L_z is computed with one of set of parameters listed in Table 3.*

B.2.2. Relative Zenith Luminance

We refer *II.a* to the approach for estimation relative zenith luminance from the second step of the algorithm for the images with overcast skies described in the paper Light Metering with Digital Cameras.

We consider two additional approaches and compare their performance.

II.b Instead of comparing the optimal vector ρ_{est} of sky parameters with a vector of parameters describing certain type of a sky, we can take the camera zenith $\theta_{c_{\text{est}}}$ and azimuth $\phi_{c_{\text{est}}}$ angles as exact. Then, for each sky type i the problem formulated on the first step of the algorithm can be solved with θ_c, ϕ_c and ρ set to $\theta_{c_{\text{est}}}, \phi_{c_{\text{est}}}$ and ρ_i. The sky type i_{opt} can then be determined as one for which the value of the objective function of the problem from the first step in the solution is minimal.

II.c In some cases, specifically when the camera is facing away from the sun, only the zenith angle of the camera θ_c

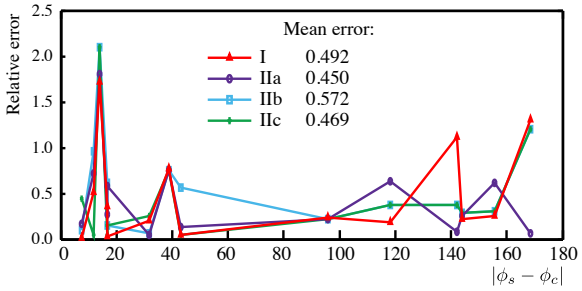

Figure 4: *Relative errors for images with overcast skies as function of the azimuth difference between sun and camera. Here we compare various algorithms that estimate the type of overcast sky. For step I, we used $l_z \leftarrow l_{z_{est}}$ in conjunction with an estimate for L_z obtained using step IIa.*

plays an important role in the calculations while errors in the azimuth angle ϕ_c do not affect the accuracy of the result. To cover this scenario, we also consider the case when $\theta_{c_{\text{est}}}$ is assumed to be an exact value of the zenith angle. In this case, we fit the value of the camera azimuth angle ϕ_c in the process of solving the indicated problem for each sky type i.

A comparison of relative errors for scale factors estimated using approaches II.a, b or c is shown in Figure 4. Approach II.a gives the lowest overall error. Moreover, this approach requires fewer computations than II.b and c.

C. Evaluation

This section contains additional details pertaining to the evaluation of our algorithm. Key results are included in the paper, while below the complete analysis is shown.

C.1. Scale Factor Estimation From EXIF Data

Under some assumptions on the camera properties, such as the lens transmittance and the vignetting factor values, used definition of sensitivity and camera metering mode one could get an approximation of light conditions. In this section we describe different approaches and discuss why these approaches could not be used as reliable algorithms in estimation of absolute data. We compare these approaches with our algorithm.

C.1.1. Scene Radiance to Irradiance in the Camera Sensor

An incoming scene radiance L is transformed by the optical system into the focal plane exposure H which is proportional to the integration time t, but decreases with the f-number N of the lens

$$H = Et = \left(q\frac{L}{N^2}\right)t, \tag{12}$$

where E is an irradiance which arrives to the camera sensor, q is a proportionality factor which could be derived as follows.

Let A_s be an area on an object surface, A_i be an area on the image plane. Then, ω_s is a solid angle subtended by area A_s and ω_i is a solid angle subtended by area A_i. Let's denote the line connecting the area on the object with the area on the image plane and passing through the lens center as r. Then, an angle α is the angle between the line r and the line perpendicular to the image plane. An angle θ is the angle between the line r and normal to the area A_s. Let's denote the distance between object surface and lens as z and the focal length as f.

To derive the connection between the scene radiance L and the irradiance E which arrives to the camera sensor the principal of radiance invariance could be used. The flux coming from the object area A_s is given by

$$\Phi_i(s) = \int_{A_s}\left(\int_{\Omega_l} L_o(s,\omega_o)\cos\alpha d\sigma_s(\omega_o)\right)d\mu^2(s), \tag{13}$$

where Ω_l is the solid angle subtended by the lens as seen from A_s, $d\mu^2(s)$ is a differential area within the area A_s. Expressing Ω_l in terms of area of lens A_l, we get

$$\begin{aligned}\Phi_i(s) &= \int_{A_s}\left(\int_{A_l} L_o(s\to l)\frac{\cos\alpha}{(z/\cos\alpha)^2}d\mu^2(l)\right)d\mu^2(s)\\ &= \{L_o(s\to l) = L_i = const\}\\ &= (A_s\cos\theta)L_i\frac{(\cos\alpha)^3}{z^2}\left(\frac{\pi d^2}{4}\right),\end{aligned} \tag{14}$$

where l is a point on the camera lens, and $d\mu^2(l)$ is a differential area on the camera lens, d is a diameter of a lens.

Then, assuming that the radiant power flows lossless through lens, from the definition an irradiance at pixel i can be written as

$$E_i = \frac{d\Phi_i}{dA_i} = \frac{\pi}{4}L_i\frac{dA_s}{dA_i}\left(\frac{d}{z}\right)^2\cos\theta(\cos\alpha)^3. \tag{15}$$

In general case this equation also includes transmittance T of the lens and the vignetting factor $v(\alpha)$:

$$E_i = \frac{d\Phi_i}{dA_i} = \frac{\pi}{4}Tv(\alpha)L_i\frac{dA_s}{dA_i}\left(\frac{d}{z}\right)^2\cos\theta(\cos\alpha)^3. \tag{16}$$

Using equality of solid angles $d\omega_s$ and $d\omega_i$:

$$\frac{dA_s\cos\alpha_s}{(z/\cos\theta)^2} = \frac{dA_i\cos\alpha}{(f/\cos\alpha)^2}, \tag{17}$$

we get

$$\frac{dA_s}{dA_i} = \frac{\cos\alpha}{\cos\theta}\left(\frac{z}{f}\right)^2. \tag{18}$$

From this and definition of f-number $N = f/d$ the final relation between L and E is

$$E_i = \frac{d\Phi_i}{dA_i} = \frac{\pi}{4}Tv(\alpha)L_i\frac{(\cos\alpha)^4}{N^2}. \tag{19}$$

Generally it's assumed that $T = 0.9$, $\alpha \in [6^o\ 10^o]$ and $v = 0.98$ and thus

$$q = \frac{\pi}{4} T v(\alpha) \in [0.65\, 0.6777]. \quad (20)$$

When the exposure is chosen automatically by a camera the vales of H depends on used definition of sensitivity as well as the camera metering mode.

C.1.2. Exposure Based on Sensitivity S

ISO standard 12232 [ISO06] includes several definitions of sensitivity. Usually it is not apparent from the available meta-data which definition was used. This can lead to greatly differing exposures for the same pixel value [AG13]. The two main way of sensitivity measurements are Saturation-based Sensitivity and Standard Output Sensitivity.

Sensitivity could be defined as

$$S = \frac{10}{H} = \frac{10}{Et}. \quad (21)$$

From (19) and (20)

$$S = 14.76\frac{N^2}{Lt}, \quad for\, \alpha = 6^o \quad (22)$$

$$S = 15.4\frac{N^2}{Lt}, \quad for\, \alpha = 10^o \quad (23)$$

Saturation-based ISO sensitivity S_{sat}. This measurement assumes the image is exposed using a standard gray card with 18 % reflectivity (r = 0.18) and that the sensor saturates (reaches its maximum output) at 141% reflectivity in order to provide some "headroom". The patch and corresponding luminance L_{sat}, where the sensor saturates is calculated by extrapolating the brightest unsaturated patches, as the saturated patches don't contain real information.

The equation connecting a radiance L and a sensitivity S is derived by assuming that the radiance of an 18% gray card $L_{0.18}$ is 18/141 of the value that saturates the sensor, L_{sat}

$$L_{0.18} = (18/141.4)L_{sat} = 0.1276 L_{sat}. \quad (24)$$

Using the form (22) of an equation (19) one can get

$$S_{sat} = 14.76\frac{N^2}{Lt} = 116\frac{N^2}{L_{sat}t}. \quad (25)$$

Standard Output Sensitivity S_{SOS}. This measurement assumes the image is exposed using a standard gray card with 18% reflectivity (r = 0.18), and that the normalized pixel level for this region is $0.18^{(1/\gamma)}$, where γ is the display gamma corresponding to the color space.

Many standard color spaces such as sRGB and Adobe RGB are designed for display with $\gamma = 2.2$. In this case the normalized pixel level is 0.4586, what is the same as the pixel level equal to 116 for 8-bit pixels where the maximum is 255. The value 0.461 or pixel level 118 is used in DC-004 because sRGB gamma is not exactly 2.2. The standard

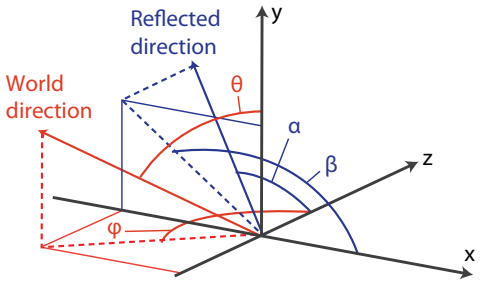

Figure 5: *Angular map parametrization.*

output sensitivity is defined as

$$S_{SOS} = 14.76\frac{N^2}{L_{0.18}t}. \quad (26)$$

As discussed in [AG13] using the different definitions of sensitivity to the same pixel in their example they get two estimations one is 1.43 times exceeds another one.

C.1.3. Exposure Based on the Reflected Light Meter Calibration Constant

Typically, the equation connecting the irradiance L and the sensitivity S has the form:

$$S = K\frac{N^2}{Lt}. \quad (27)$$

The constant K frequently call the in camera reflected-light meter calibration constant which depends on camera. The common choice of this constant is $K = 12.5$.

C.1.4. Absolute Data Estimation

The scale factor for the image could be found from the equations of the form (27) with an appropriate value of K under assumptions: that the mean luminance in the area measured by in-camera light meter corresponds to the luminance of 18% card if this card would be inserted into the scene and measured; one of two described above definitions of the sensitivity. The first assumption leads to the higher errors in case of high dynamic range scenes.

Ackermann et al. [AG13] suggested the modification of this equation which account for gamma curve of sRGB color space. The radiance value L_p for each pixel p with intensity value I_p can be found from an equation:

$$L_p = 15.4\frac{f^{-1}(I_p/255)}{f^{-1}(118/255)}\frac{N^2}{S_{SOS}t}, \quad (28)$$

where f^{-1} corresponds to the inverse gamma correction of sRGB color space.

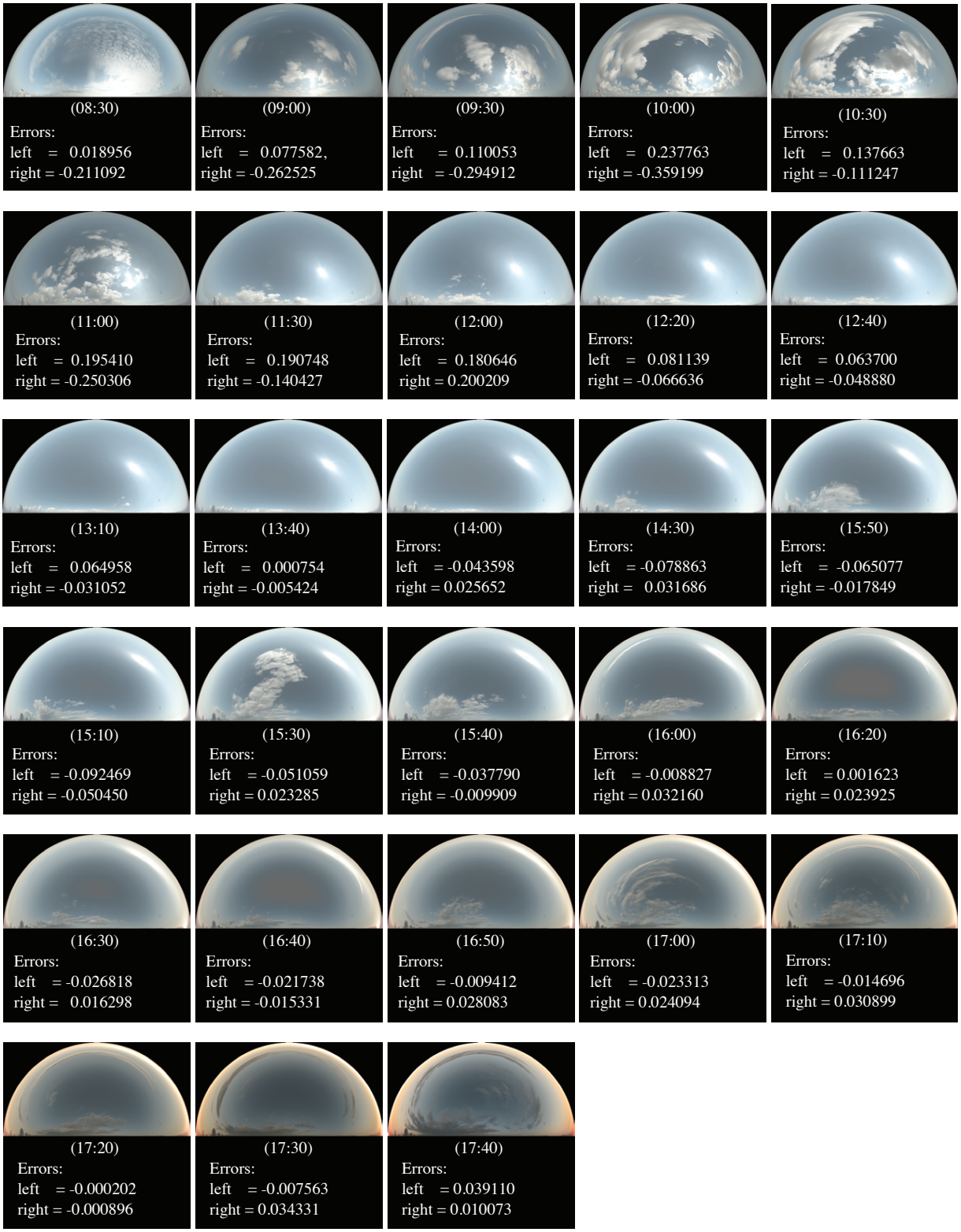

Figure 6: *Relative errors for each of sky probe*

References

[AG13] ACKERMANN J., GOESELE M.: *Computational Color Imaging*, vol. LNCS7786. Springer, 2013, ch. How Bright Is the Moon? Recovering and Using Absolute Luminance Values from Internet Images. 6

[CIE03] CIE: *Spatial distribution of daylight — CIE standard general sky*. CIE Standard S 011/E:2003CIE Central Bureau, Vienna, 2003. 3

[Fai07] FAIRCHILD M.: The HDR photographic survey. In *Proc. of the 15th IS&T Color Imaging Conference* (2007), pp. 233–238. 4

[HW12] HOSEK L., WILKIE A.: An analytic model for full spectral sky-dome radiance. *ACM Trans. Graph. 31*, 4 (July 2012), 95:1–95:9.

[IM94] INEICHEN P., MOLINEAUX B.: Sky luminance data validation: Comparison of 7 models with 4 data banks. *Solar Energy 52*, 4 (1994), 337–346. 1

[ISO06] ISO: *Photography - digital still cameras - determination of exposure index, iso speed ratings, standard output sensitivity, and recommended exposure index*, 2006. 6

[KNNS84] KARAYEL M., NAVVAB M., NEEMAN E., SELKOWITZ S. E.: Zenith luminance and sky luminance distributions for daylighting calculations. *Energy And Buildings 6*, 3 (1984), 283–291. 3

[KPD98] KITTLER R., PEREZ R., DARULA S.: *A set of standard skies characterizing daylight conditions for computer and energy conscious design*. US SK 92 052 Final Report, CA SAS Bratislava, 1998. 3

[LGE10] LALONDE J.-F., G. N. S., EFROS A. A.: What do the sun and the sky tell us about the camera? *International Journal of Computer Vision 88*, 1 (2010), 24–51. 2

[LNE08] LALONDE J.-F., NARASIMHAN S. G., EFROS A. A.: What does the sky tell us about the camera? In *Proc. of ECCV* (2008), pp. 354–367. 2

[McC76] MCCARTNEY E. J.: *Optics of the Atmosphere: Scattering by molecules and particles*. John Wiley & Sons, New York, 1976. 1

[PSM93] PEREZ R., SEALS R., MICHALSKY J.: All-weather model for sky luminance distribution-preliminary configuration and validation. *Solar Energy 50*, 3 (1993), 235–245. 1, 3

[PSS99] PREETHAM A. J., SHIRLEY P., SMITS B.: A practical analytic model for daylight. In *Proc. of SIGGRAPH '99* (1999), ACM Press/Addison-Wesley Publishing Co., pp. 91–100. 2, 3

[RHD*10] REINHARD E., HEIDRICH W., DEBEVEC P., PATTANAIK S., WARD G., MYSZKOWSKI K.: *High Dynamic Range Imaging: Acquisition, Display and Image-Based Lighting*, 2nd ed. Morgan Kaufmann, San Francisco, 2010.

[SG00] SOLER A., GOPINATHAN K. K.: A study of zenith luminance on Madrid cloudless skies. *Solar Energy 69*, 5 (2000), 403–411. 3, 4

[SG01] SOLER A., GOPINATHAN K. K.: Analysis of zenith luminance data for all sky conditions. *Renewable Energy 24*, 2 (2001), 185–196. 3

[SGC01] SOLER A., GOPINATHAN K. K., CLAROSA S.: A study on zenith luminance on Madrid overcast skies. *Renewable Energy 23*, 1 (2001), 49–55. 3

[STJ*04] STUMPFEL J., TCHOU C., JONES A., HAWKINS T., WENGER A., DEBEVEC P.: Direct HDR capture of the sun and sky. In *Proc. of Afrigraph* (2004), ACM, pp. 145–149.

[ZWP07] ZOTTI G., WILKIE A., PURGATHOFER W.: A critical review of the Preetham skylight model. In *WSCG 2007 Short Communications Proceedings I* (2007), pp. 23–30. 3